Physica D 443 (2023) 133564

Contents lists available at ScienceDirect

Physica D

journal homepage: www.elsevier.com/locate/physd

Magnon–lattice dynamics in a Heisenberg–Morse model with spin–lattice interaction

M.O. Sales [a], A. Ranciaro Neto [b], F.A.B.F. de Moura [c,*]

[a] IFMA Campus São João dos Patos, rua Padre Santiago, s/n, Centro, São João dos Patos MA, 65665-000, Brazil
[b] Faculdade de Economia, Administração e Contabilidade, Universidade Federal de Alagoas, Maceió AL 57072-970, Brazil
[c] Instituto de Física, Universidade Federal de Alagoas, Maceió AL 57072-970, Brazil

ARTICLE INFO

Article history:
Received 26 May 2022
Received in revised form 3 September 2022
Accepted 14 October 2022
Available online 25 October 2022
Communicated by S. Wang

Keywords:
Magnon–soliton pair
Magnon propagation
Soliton
Morse lattice

ABSTRACT

We investigate the dynamics of a single magnon excitation in a quantum Heisenberg model under the effect of lattice vibrations. The Heisenberg spins are set on a nonlinear Morse chain, with the coupling depending on their distance. We solve the time evolution numerically and discuss the magnon velocity's dependence on the spin–lattice coupling. Our results show that the lattice deformation embodies a finite fraction of the spin wave function in the robust spin–lattice coupling regime, generating a mobile magnon–lattice excitation. We also analyze the lattice deformation and magnon wave functions separately. Our results indicate both spatial profiles display solitonic features.

© 2022 Elsevier B.V. All rights reserved.

1. Introduction

The relationship between particle, energy transport and their embedded lattice structure has always drawn a great deal of attention in several contexts [1–24]. In terms of electronic propagation, the famous work done by Su, Schrieffer, and Heeger (SSH) [4] was used to study the conductivity of trans-polyacetylene. They employed a one-dimensional tight-binding Hamiltonian in which the off-diagonal terms depended on the spatial structure of the polyacetylene. Quantum simulation of the SSH model was implemented using an atom-optics setup in [5].

A number of works showed that electron–lattice coupling provides with electronic propagation [25–29]. Other studies on charge transportation in nonlinear chains addressed the existence of a quasi-particle emerging from the coupling between self-trapped (polaron) states and lattice solitons [30–40]. For instance, in Ref. [40], it was shown that a mobile discrete breather–electron coupling promotes charge transport. In a fine experiment described in Ref. [41], controlled electronic dynamics were obtained using electron-lattice interaction. The setup consisted of a single electron trapped in a quantum dot, moving around a channel via surface acoustic wave (SAW) [42–51]. The authors in Ref. [52] provided a comprehensive review of many other ways to gain control over a propagating single-electron. Potential applications to quantum information processing are also discussed.

The problem of magnetic excitations interacting with lattice vibrations have also attracted interest [53–70]. In Ref. [54] the authors demonstrate that SAW can control the magnetization of a ferromagnetic Ni film. The thermal Hall effect is controlled by magnon–phonon coupling was described on a ferromagnetic square lattice featuring Dzyaloshinskii–Moriya interaction [57]. Ref. [58] reported signals of collective antiferromagnetic magnon-phonon dynamics in an insulator Cr_2O_3. It was shown in [59] that the magnon–phonon coupling could amplify spin pumping in a Pt/YIG bi-layer film.

As we can see, magnon propagation dynamics mediated by lattice interaction is a relevant topic. Inspired by this, we study magnon dynamics in a quantum Heisenberg model featuring lattice vibrations considering a nonlinear Morse chain. Spin exchange interactions between nearest-neighbor sites are set as a function of their distance. To keep track of the magnon dynamics, we solve the differential equations numerically using a Taylor formalism combined with a second-order Euler procedure. Our results show that strong magnon–lattice interaction yields collective magnon–soliton dynamics. The magnon velocity depends on the magnon–lattice coupling. We also address the overlap between the localized magnon wave input and solitonic modes. Magnon–soliton hybrid excitations are shown to collide with minimum interference.

In this work, the problem involving dynamics of magnon excitation in a Morse lattice are investigated considering the Heisenberg model in a Morse Lattice. In our model, the spin–spin coupling is directly connected with the lattice deformation. By using numerical methods to solve the quantum equation and

* Corresponding author.
E-mail address: fidelis@fis.ufal.br (F.A.B.F. de Moura).

https://doi.org/10.1016/j.physd.2022.133564
0167-2789/© 2022 Elsevier B.V. All rights reserved.

the classical vibrational problem, we investigate the existence of a magnon–soliton pair formation. We demonstrate numerically that for some specific values of magnon–lattice interaction, the magnon–lattice bound states occur with reasonable stability.

2. Model and numerical calculation

We define a quantum Heisenberg model with N spin$-1/2$ particles on a nonlinear Morse chain. Its Hamiltonian is given by [71,72]:

$$\mathcal{H}_S = -\sum_{k=1}^{N}\{J_{k,k+1}\vec{S}_k\vec{S}_{k+1}\}, \tag{1}$$

where $J_{k,k+1}$ represents the exchange interaction between sites k and $k+1$. The spin–spin interaction is set to follow

$$J_{k,k+1} = Je^{-\alpha(R_{k+1}-R_k)}, \tag{2}$$

where R_k and R_{k+1} represent the displacement of spins k and $k+1$ from their equilibrium position. The quantity α is an adjustable parameter that controls the intensity of spin–lattice coupling. The displacements $\{R_k\}$ can be found by solving the lattice dynamics represented by the classical Hamiltonian [73]

$$H_L = \sum_{k=1}^{N}\frac{P_k^2}{2M} + \sum_{k=1}^{N} Z\left\{1-exp\left[-Q(R_k-R_{k-1})\right]\right\}^2. \tag{3}$$

Here, P_k stands for the particle moment at site k and $M=1$ is the mass of each particle. We emphasize that the above Hamiltonian basically describes a chain with nearest-neighbor masses coupled by a Morse potential [73–76]. We also use the dimensionless representation by absorbing the constants Z and Q as the following [22]: $R_k \to QR_k$; $P_k \to P_k/\sqrt{2Z}$ and $H_L \to H_L/(2Z)$. The time-dependent spin wave function is $|\Phi(t)\rangle = \sum_k c_k|k\rangle$, where $|k\rangle$ denotes a single spin at the k site (i.e. $|k\rangle = S_k^-|0\rangle$ where $|0\rangle$ is the ground state). Therefore, the time-dependent Schrödinger equation can be written in the form

$$\begin{aligned} i\frac{dc_k(t)}{dt} = \frac{\tau}{2}\{&[exp(-\alpha(R_{k+1}-R_k)) \\ &+ exp(-\alpha(R_k-R_{k-1}))]c_k(t) \\ &- exp(-\alpha(R_k-R_{k-1}))c_{k-1}(t) \\ &- exp(-\alpha(R_{k+1}-R_k))c_{k+1}(t)\}. \end{aligned} \tag{4}$$

On the other hand, the classical vibrations can be obtained from the Hamilton equations, leading to

$$\begin{aligned} \frac{d^2R_k}{dt^2} = &\{1-exp[-(R_{k+1}-R_k)]\}exp[-(R_{k+1}-R_k)] \\ &- \{1-exp[-(R_k-R_{k-1})]\}exp[-(R_k-R_{k-1})] \\ &+ \frac{J\alpha}{2}\Big[e^{-\alpha(R_k-R_{k-1})}(c_k^*c_k + c_{k-1}^*c_{k-1}) \\ &- e^{-\alpha(R_{k+1}-R_k)}(c_k^*c_k + c_{k+1}^*c_{k+1}) \\ &+ e^{-\alpha(R_{k+1}-R_k)}(c_{k+1}^*c_k + c_k^*c_{k+1}) \\ &- e^{-\alpha(R_k-R_{k-1})}(c_{k-1}^*c_k + c_k^*c_{k-1})\Big]. \end{aligned} \tag{5}$$

In the above differential equations, we rescaled time as $t \to \omega t$, where ω is the frequency of oscillations around the minimum of the Morse potential [73]. We further consider $\tau = J/(\hbar\omega) = 10$ to account for the timescale difference between electronic dynamics (faster) and lattice vibrations (slower). We emphasize that value was obtained in several papers by Velarde and Davydov [25,26,73]. The authors of these papers demonstrate that quantum dynamics is about ten times faster than classical propagation. Henceforth, following Ref. [73] we consider $J = 0.1$. Within the context of the value of J we emphasize that based on several Refs. [77–80], we can see that $J \leq 0.1eV$. We also emphasize that we can understand the quantity J in our model as the typical energy unit. Thus, we can adjust the model by choosing our parameter J in units of eV. Therefore our choice to J agrees reasonably well with the typical values of J found in several materials (or models) [25,26,73,77–80]. We will discuss briefly, at the end of our work, the dependence of our model and results with the value of J.

Our calculations will be done throughout numerical solution of set of equations (4) and (5). The quantum equations (4) are solved first by writing the time evolution operator $\tilde{O}(\delta t)$ as a Taylor expansion up to $\tilde{O}(\delta t) = e^{(-iH\,S^{\delta t})} = 1+\sum_{l=1}^{n_o}(-iH_S\delta t)^l/(l!)$ [81]. The sum is truncated at $n_0 = 10$ and we use $\delta t = 2\times 10^{-3}$. The classical equations are solved using a modified Euler method defined in [82,83]. It begins by estimating $R_k(\delta t)^1 \approx R_k(t=0) + \delta t(dR_k/dt)|_{t=0}$ at time δt. We then work out improved solutions $R_k(\delta t)^2$, that is $R_k(\delta t) \approx R_k(t=0) + (\delta t/2)\left[(dR_k^1/dt)|_{t=0} + (dR_k^2/dt)|_{\delta t}\right]$. The accuracy is routinely verified by checking the wave function norm. For all the numerical simulations below, $|1-\sum_k|c_k(t)|^2| < 10^{-11}$. Considering the class of problems we deal with here, the above approach offers some advantages compared to standard methods such as the Runge–Kutta scheme.

In order to follow the dynamics of the magnon, we evaluate its mean position

$$n_S(t) = \sum_k (k-N/2)|c_k(t)|^2, \tag{6}$$

and the so-called participation number

$$P(t) = [\sum_k |c_k(t)|^4]^{-1}, \tag{7}$$

which gives 1 when the wave function is fully localized and $\sim N$ when it features an extended profile. The quantity G_k will describe the lattice behavior at the site k. G_k is a generalized probability that deformation around site k occurs. This is obtained by normalizing $u_k = (1-e^{[-R_k+R_{k-1}]})^2$, that is $G_k = u_k/\sum_k(u_k)$. This quantity allows us to compute the centroid of the lattice deformation

$$n_L(t) = \sum_k (k-N/2)G_k. \tag{8}$$

We will present our results in the following section. We fix the chain size to $N = 10^5$ sites and set the input considering $c_k(t=0) = \delta_{k,N/2}$, $\dot{R}_k(t=0) = \delta_{k,N/2}$ and $R_k(t=0) = 0$. We do not fully integrate the set of differential equations; we do it for a region around the initial position $N/2$ by taking k equations within the interval $[N/2-b/2, N/2+b/2]$, with $b = 100$ initially. When either the wave function or nonlinear vibrations reach the boundaries of that interval, we increase b. That procedure promotes computational resources optimization.

3. Results

Fig. 1(a) shows the magnon centroid $n_S(t)$ versus time for several spin–lattice coupling strengths, $\alpha = 0$ to 2. We also stress that such dependence of $n_S(t)$ with the spin–lattice coupling was also observed in Fermi–Pasta–Ulam chains [69]. The relationship between the excitation centroid and the spin–lattice coupling suggests, in general, the overlap of a finite fraction of the magnon wave function with solitonic modes. In order to dig for more details, in Fig. 1(b) we plot the centroid of both magnon and

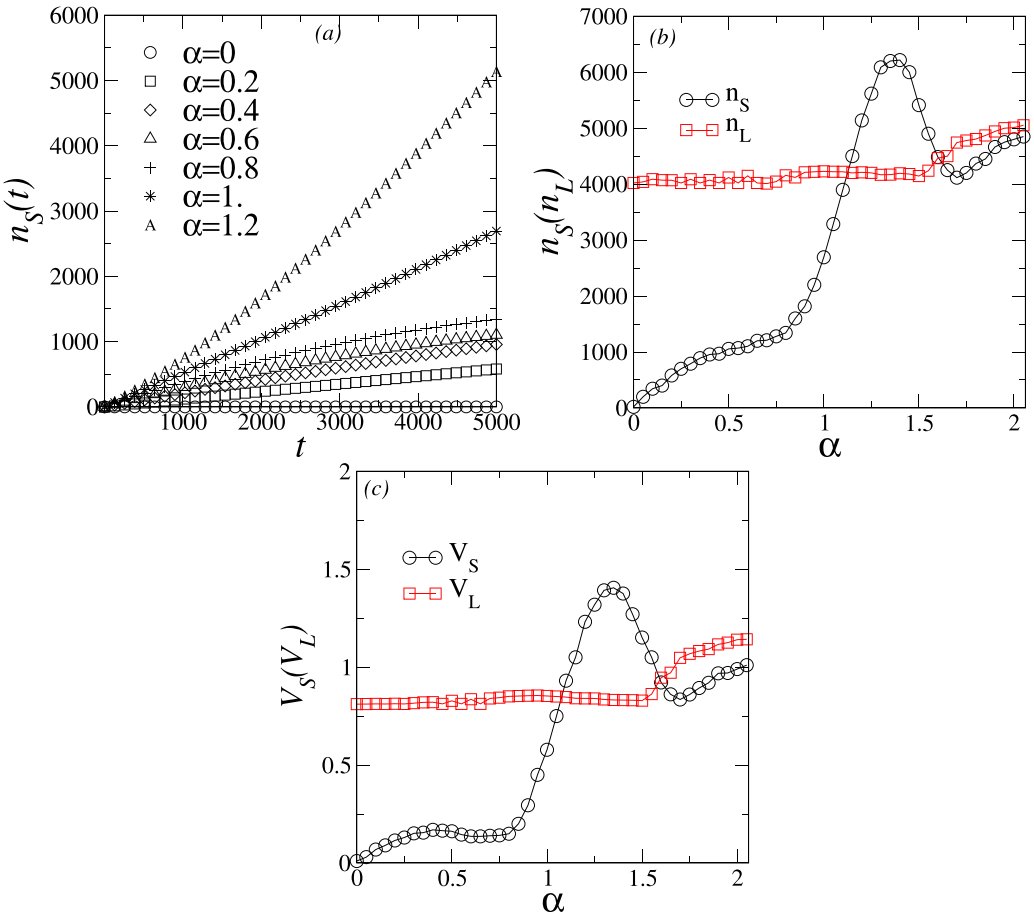

Fig. 1. (a) Mean position of the magnon $n_S(t)$ versus time for several values of spin–magnon interaction α. (b) Mean position of the magnon alongside lattice deformation's, n_L versus α. (c) Magnon and lattice deformation velocities V_S and V_L, respectively, versus α.

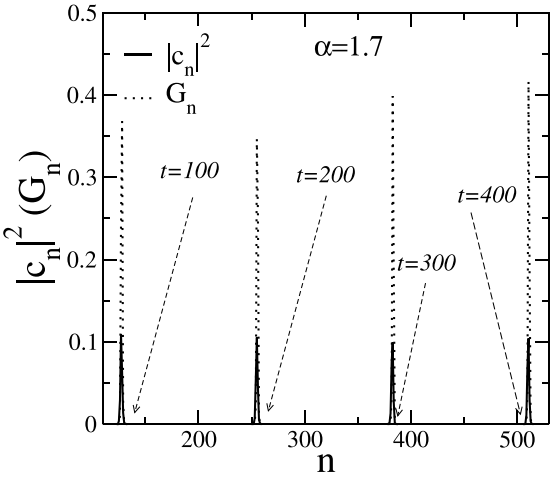

Fig. 2. Two-dimensional profile of the wave function ($|c_n|^2 \times n$; solid line) and lattice deformation probability $G_n \times n$ (dotted lines) at $t = 100, 200, 300, 400$. For both quantities we set $n = k - N/2$ and fix $\alpha = 1.7$.

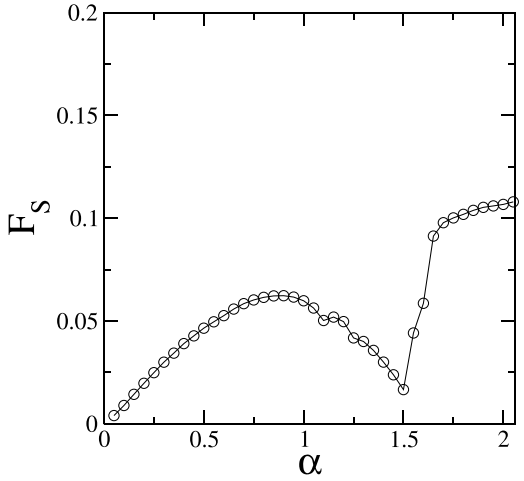

Fig. 3. Fraction of the magnon wave function trapped by the lattice deformation F_S measures in the long time limit. Calculations suggest that for $\alpha > 1.6$ the fraction of the wave function trapped by the solitonic deformations remains roughly stable.

lattice deformation excitations at the long-time limit, that is $n_S = n_S(t \to t_{max})$ and $n_L = n_L(t \to t_{max})$. Additionally, in Fig. 1(c) we show their propagation speeds, V_S and V_L, respectively versus α, obtained via linear regression of $n_S(t)$ and $n_L(t)$ for $t \to t_{max} = 5 \times 10^3$. We see that both excitations remain separated depending on the spin–lattice coupling strength (when $\alpha = 1.4$, for instance). Moreover, their position and velocity values are very close to some specific values.

Let us now monitor the wave function's shape along the time to understand the interaction between magnon and lattice deformation and to analyze magnon–lattice pair formation. In Fig. 2 we plot both $|c_n|^2 \times n$ and the lattice deformation probability

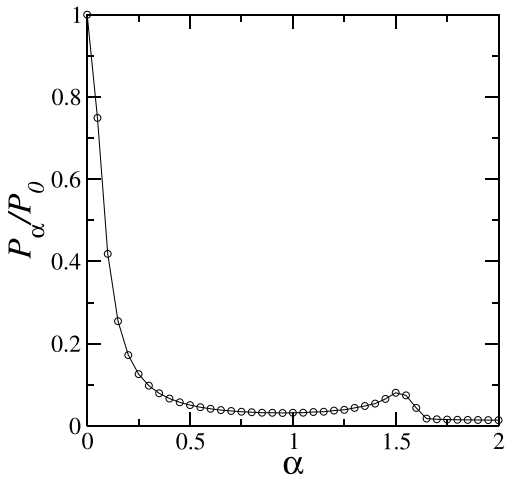

Fig. 4. Scaled participation number in the long time limit $P_\alpha/P_0 = P(\alpha, t \to t_{max})/P_0$ versus α. We see that lattice deformation promotes the trapping of a finite fraction of the magnon wave packet for $\alpha > 1.6$.

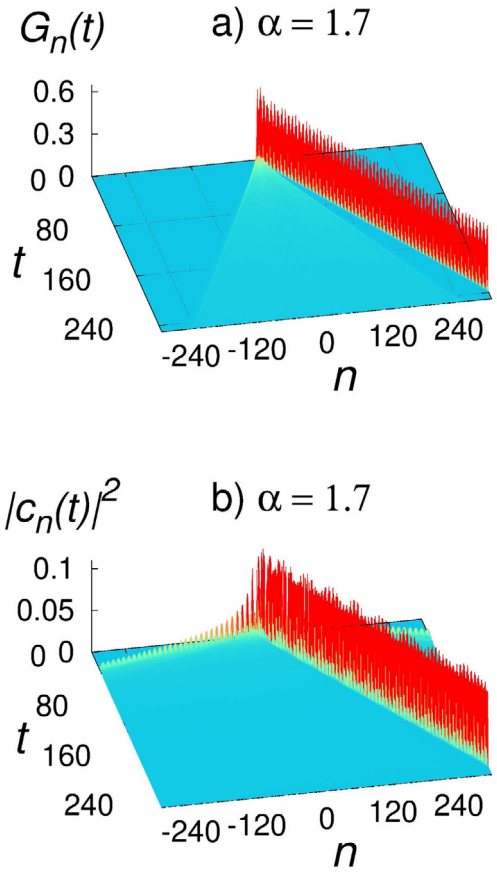

Fig. 5. (a) Lattice deformation $G_n(t)$ and (b) occupation probability $|c_n(t)|^2$ for the magnon initially localized at site $n = k - N/2 = 0$ and lattice featuring velocity $\dot{R}_n(t = 0) = \delta_{n,0}$.

$G_n \times n$ at different times. We emphasize that $n = k - N/2$. We see the magnon gets trapped by the solitonic mode, as told by the perfect match of the dotted lines (soliton shape) and the solid line (magnon shape). To see how that goes with α, in Fig. 3 we track how much of the magnon wave function was trapped by the solitonic lattice deformation, F_S, in the long time limit. In practical terms, we follow the position of the lattice wave and evaluate the magnon occupation probability at the same spot. It is remarkable

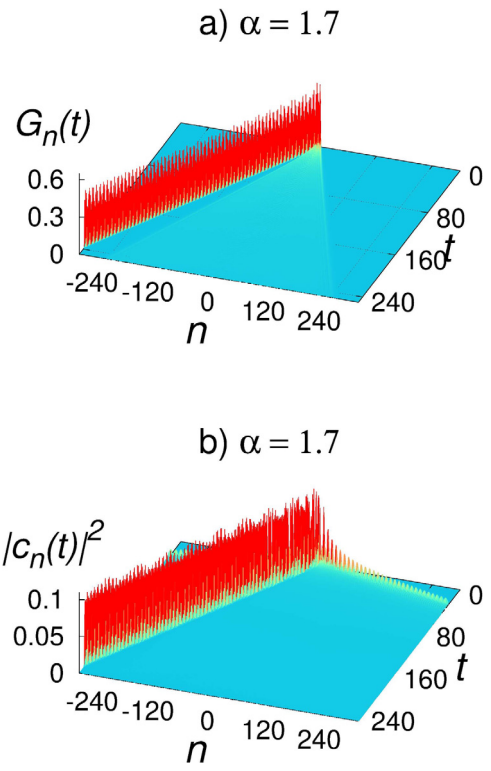

Fig. 6. (a) Lattice deformation $G_n(t)$ and (b) occupation probability $|c_n(t)|^2$ for the magnon initially localized at site $n = k - N/2 = 0$ and lattice featuring velocity $\dot{R}_n(t = 0) = -\delta_{n,0}$.

what happens to it when $\alpha > 1.6$. Calculations suggest that for $\alpha > 1.6$ the fraction of the wave function trapped by the solitonic deformations remains roughly constant. For $\alpha \approx 1.5$, we can see that the fraction of the wave function captured by the solitonic mode decreases. We do not know precisely the explanation for the non-monotonic dependence of F_S with α. However, we can provide a brief discussion about this crucial point. The parameter α represents the intensity of the magnon–lattice interaction. Therefore, by changing α, we are changing the kind of dynamics disorder within the spin–spin coupling distribution. This dynamic disorder's scattering of the magnon wave function is a nontrivial process, and some destructive (or constructive) internal interference can contribute to trap the wave function. At this point, it is convenient to analyze those features in light of the degree of magnon localization. In Fig. 4, we show the scaled participation number in the long time limit i.e. $P_\alpha/P_0 = P(\alpha, t \to t_{max})/P_0$. We emphasize that $P_0 = P(\alpha = 0, t \to t_{max})$ is the participation number in the long time limit in the absence of magnon–lattice interaction($\alpha = 0$). We see that it exhibits a large participation number for $\alpha \approx 0$ and become more localized as α is increased. When $\alpha > 1.6$, the participation number declines rapidly. The decrease in the participation number is related to the trapping of the wave function by the lattice deformation.

Now, we investigate the role of different types of initial conditions. In Fig. 5, we plot the lattice deformation $G_n(t)$ and wave function $|c_n(t)|^2$ versus n and t considering $\alpha = 1.7$. Therein we see their solitonic profile, as expected. It is also interesting to note that magnon wave function travels roughly with the velocity predicted earlier. We emphasize that $n = m - N/2$, with the magnon initially at $n = 0$. The lattice properties are $\dot{R}_n(t = 0) = \delta_{n,0}$ and $R_n(t = 0) = 0$. (For now, this configuration is the same as in the previous figures.) Another aspect worth pointing out in Fig. 5(b) is that small-amplitude irradiation goes outwards at

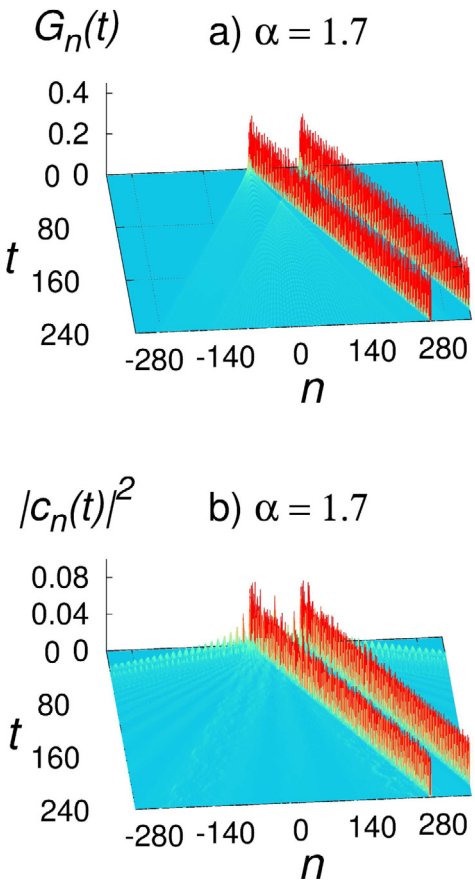

Fig. 7. (a) Lattice deformation $G_n(t)$ and (b) occupation probability $|c_n(t)|^2$ with the magnon initially set as $c_n(t=0) = \frac{1}{\sqrt{2}}\delta_{n,-n_0} + \frac{1}{\sqrt{2}}\delta_{n,n_0}$ and lattice velocity $\dot{R}_n(t=0) = \delta_{n,-n_0} + \delta_{n,n_0}$, with $n_0 = 50$. We stress that $n = k - N/2$.

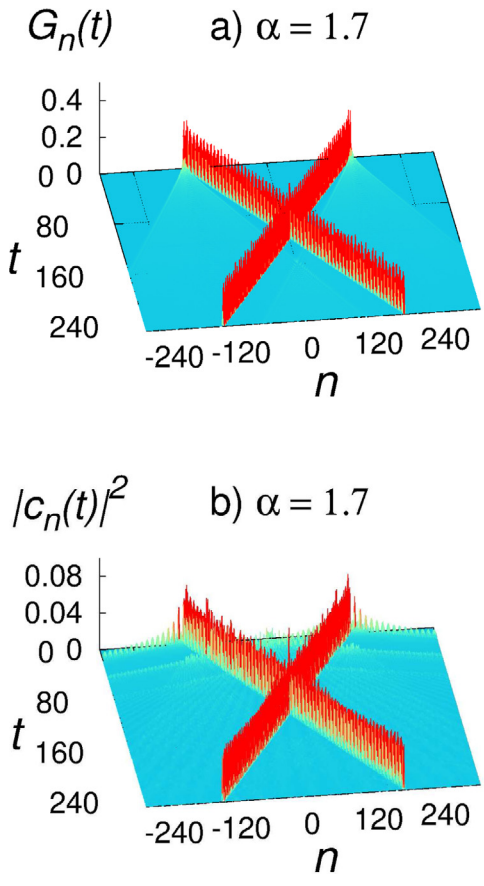

Fig. 8. (a) Lattice deformation $G_n(t)$ and (b) occupation probability $|c_n(t)|^2$ with the magnon initially set as $c_n(t=0) = \frac{1}{\sqrt{2}}\delta_{n,-n_0} + \frac{1}{\sqrt{2}}\delta_{n,n_0}$ and lattice velocity $\dot{R}_n(t=0) = \delta_{n,-n_0} - \delta_{n,n_0}$, with $n_0 = 150$. We stress that $n = k - N/2$.

initial times. Similar processes were reported in the context of electron–soliton dynamics. The critical point here is that whereas the solitonic deformation mode captures a finite fraction of the initial wave function, the remaining part propagates freely. In Fig. 6 we change the initial velocity of the lattice component to $\dot{R}_n(t=0) = -\delta_{n,0}$. The solitonic mode is also produced whenever the Morse lattice is initialized through an impulse with negative velocity. This time, however, it goes the other way around. It should be clear that the results reported in Figs. 1 through 3 are qualitatively the same as those obtained in the case of initial negative velocity.

Figs. 7 and 8 show the dynamics for rather different initial conditions. Now, the magnon wave function is set with $c_n(t = 0) = \frac{1}{\sqrt{2}}\delta_{n,-n_0} + \frac{1}{\sqrt{2}}\delta_{n,n_0}$ lattice velocity as $\dot{R}_n(t = 0) = v_1\delta_{n,-n_0} + v_2\delta_{n,n_0}$. In Fig. 7 we consider $n_0 = 50$ and $v_1 = v_2 = 1$. In this case, we observe two lattice deformation solitonic modes (one at each impulse input location). Once again, each of these captures a finite fraction of the magnon wave function that, likewise, spreads out carrying the same solitonic profile. In Fig. 8 we consider $n_0 = 150$ and $v_1 = -v_2 = 1$. This time the solitons move towards each other (due to the initial velocities with opposite signals). After a while, a collision takes place in both components. After that, both pulses retain their trajectory and shape. We stress that this collision without any apparent destruction of the solitonic shape is a key signature that a magnon–soliton pair indeed takes place at the regime of strong magnon elastic coupling ($\alpha > 1.6$). Before concluding our work, we will briefly discuss our main results' dependence on

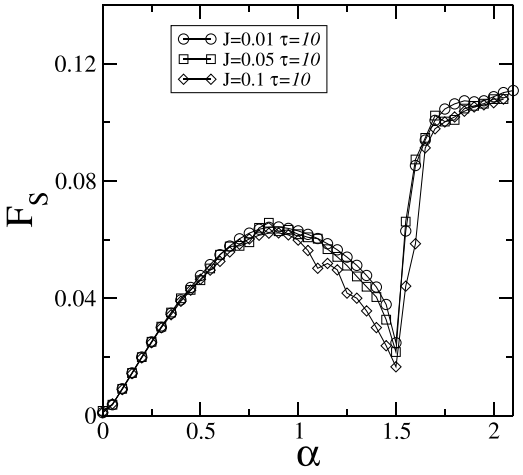

Fig. 9. The fraction of the magnon wave function trapped by the lattice deformation F_S versus α considering $J = 0.01, 0.05, 0.1$.

the value of J. We stress that, in a wide range of materials [77–80], J was obtained about $0.01eV$ up to $0.1eV$. Therefore we will compare the behavior of the quantity $F_S(\alpha)$ considering these values $J = 0.01$ up to 0.1. In Fig. 9 we plot the quantity F_S versus α considering $J = 0.01, 0.05, 0.1$. Our calculations indicate that the main results are roughly the same: for $\alpha \geq 1.6$, the solitonic mode captures a finite fraction of the magnon wave function.

4. Final remarks

We have investigated the magnon dynamics on a nonlinear Morse chain, where the spin–spin coupling depends on their distance. By setting up an impulse excitation at the mass located at the center of the chain, it is possible to induce the appearance of a solitonic lattice mode which, depending on the spin–lattice coupling strength, is capable of carrying part of the magnon wave function along. We carried out detailed numerical investigations and found that in the regime of the spin–lattice strong interaction, a stable hybrid magnon–soliton excitation takes place. Moreover, depending on the initial conditions, we can bring about more of those structures, study collisions etc. We found that after colliding, both pulses remained unchanged, adding evidence for the robustness of those solitonic modes. Further studies may be conducted to test such stability against static and dynamical fluctuations to account for more realistic settings.

CRediT authorship contribution statement

M.O. Sales: Conceptualization, Methodology, Software, Calculations. **A. Ranciaro Neto:** Numerical calculations, Validation, Reviewing. **F.A.B.F. de Moura:** Conceptualization, Methodology, Numerical calculations, Writing – review & editing.

Declaration of competing interest

The authors declare that they have no known competing financial interests or personal relationships that could have appeared to influence the work reported in this paper.

Data availability

Data will be made available on request.

Acknowledgments

We thank GMA Almeida for a careful reading of the manuscript. This work was supported by CNPq, Brazil, CAPES, Brazil, FINEP (Federal Brazilian Agencies), and FAPEAL (Alagoas State Agency).

References

[1] F.A.B.F. de Moura, Physica D 253 (2013) 66–72.
[2] A.P. Chetverikov, W. Ebeling, E. del Rio, K.S. Sergeev, M.G. Velarde, Chaos Solitons Fractals 150 (2021) 111179.
[3] I.A. Shepelev, S.V. Dmitriev, A.A. Kudreyko, M.G. Velarde, E.A. Korznikova, Chaos Solitons Fractals 140 (2020) 110217.
[4] W.P. Su, J.R. Schrieffer, A.J. Heeger, Phys. Rev. Lett. 42 (1979) 1698;
W.P. Su, J.R. Schrieffer, A.J. Heeger, Phys. Rev. B 22 (1980) 2099;
A.J. Heeger, S. Kivelson, J.R. Schrieffer, P. W.-Su, Rev. Mod. Phys. 60 (1988) 781.
[5] E. Meier, F. An, B. Gadway, Nat. Commun. 7 (2016) 13986.
[6] C. Skokos, D.O. Krimer, S. Komineas, S. Flach, Phys. Rev. E 79 (2009) 056211;
C. Skokos, D.O. Krimer, S. Komineas, S. Flach, Phys. Rev. E 89 (2014) 029907;
D. Leykam, S. Flach, O. Bahat-Treidel, A.S. Desyatnikov, Phys. Rev. B 88 (2013) 224203;
G. Gligorić, K. Rayanov, S. Flach, EPL 101 (2013) 10011;
T.V. Laptyeva, J.D. Bodyfelt, S. Flach, EPL 98 (2012) 60002;
M. Larcher, T.V. Laptyeva, J.D. Bodyfelt, F. Dalfovo, M. Modugno, S. Flach, New J. Phys. 14 (2012) 103036.
[7] Ch. Skokos, S. Flach, Phys. Rev. E 82 (2010) 016208.
[8] M.V. Ivanchenko, T.V. Laptyeva, S. Flach, Phys. Rev. Lett. 107 (2011) 240602.
[9] Ch. Skokos, I. Gkolias, S. Flach, Phys. Rev. Lett. 111 (2013) 064101.
[10] J.D. Bodyfelt, T.V. Laptyeva, G. Gligoric, D.O. Krimer, Ch. Skokos, S. Flach, Int. J. Bifurcation Chaos 21 (2011) 2107–2124.
[11] S. Flach, Springer Proc. Phys. 173 (2016) 45.
[12] T.V. Laptyeva, M.V. Ivanchenko, S. Flach, J. Phys. A 47 (2014) 493001.
[13] A. Pikovsky, J. Stat. Mech. Theory Exp. (2015) P08007.
[14] F.A.B.F. de Moura, I. Gléria, I.F. dos Santos, M.L. Lyra, Phys. Rev. Lett. 103 (2009) 09640.
[15] G. Kopidakis, S. Komineas, S. Flach, S. Aubry, Phys. Rev. Lett. 100 (2008) 084103;
A.S. Pikovsky, D.L. Shepelyansky, Phys. Rev. Lett. 100 (2008) 094101;
D. Hajnal, R. Schilling, Phys. Rev. Lett. 101 (2008) 124101;
Y. Lahini, A. Avidan, F. Pozzi, M. Sorel, R. Morandotti, D.N. Christodoulides, Y. Silberberg, Phys. Rev. Lett. 100 (2008) 013906.
[16] J.-K. Xue, A.-X. Zhang, Phys. Rev. Lett. 101 (2008) 180401;
N. Akhmediev, A. Ankiewicz, J.M. Soto-Crespo, Phys. Rev. E 80 (2009) 026601;
S.A. Ponomarenko, G.P. Agrawal, Phys. Rev. Lett. 97 (2006) 013901;
A. Maluckov, L.j. Hadzievski, N. Lazarides, G.P. Tsironis, Phys. Rev. E 79 (2009) 025601, (R);
Y. Lahini, A. Avidan, F. Pozzi, M. Sorel, R. Morandotti, D.N. Christodoulides, Y. Silberberg, Phys. Rev. Lett. 100 (2008) 013906;
T.h. Anker, M. Albiez, R. Gati, S. Hunsmann, B. Eiermann, A. Trombettoni, M.K. Oberthaler, Phys. Rev. Lett. 94 (2005) 020403.
[17] J.E. Macías-Díaz, I.E. Medina-Ramírez, Commun. Nonlinear Sci. Numer. Simul. 14 (2009) 3200.
[18] T. Dauxois, M. Peyrard, S. Ruffo, Eur. J. Phys. 26 (2005) S3–S11.
[19] L. Brizhik, A.P. Chetverikov, W. Ebeling, G. Ropke, M.G. Velarde, Phys. Rev. B 85 (2012) 245105.
[20] A.P. Chetverikov, W. Ebeling, M.G. Velarde, Physica D 240 (2011) 1954.
[21] D. Hennig, M.G. Velarde, W. Ebeling, A.P. Chetverikov, Phys. Rev. E 78 (2008) 066606.
[22] D. Hennig, A. Chetverikov, M.G. Velarde, W. Ebeling, Phys. Rev. E 76 (2007) 046602.
[23] V.A. Makarov, M.G. Velarde, A.P. Chetverikov, W. Ebeling, Phys. Rev. E 73 (2006) 066626.
[24] D. Hennig, C. Neissner, M.G. Velarde, W. Ebeling, Phys. Rev. B 73 (2006) 024306.
[25] A.S. Davydov, Solitons in Molecular Systems, second ed., Reidel, Dordrecht, 1991.
[26] A.C. Scott, Phys. Rep. 217 (1992) 1–67.
[27] A.S. Davydov, Phys. Scripta 20 (1979) 387–394.
[28] A.S. Davydov, J. Theoret. Biol. 66 (1977) 379–387.
[29] A.S. Davydov, Biology and Quantum Mechanics, Pergamon, New York, 1982.
[30] B.J. Alder, K.J. Runge, R.T. Scalettar, Phys. Rev. Lett. 79 (1997) 3022.
[31] L.S. Brizhik, A.A. Eremko, Physica D 81 (1995) 295–304.
[32] O.G. Cantu Ross, L. Cruzeiro, M.G. Velarde, W. Ebeling, Eur. Phys. J. B 80 (2011) 545–554.
[33] A.P. Chetverikov, W. Ebeling, M.G. Velarde, Eur. Phys. J. B 80 (2011) 137–145.
[34] D. Hennig, M.G. Velarde, W. Ebeling, A. Chetverikov, Phys. Rev. E 78 (2007) 066606.
[35] M.G. Velarde, W. Ebeling, A.P. Chetverikov, Internat. J. Bifur. Chaos 15 (2005) 245.
[36] M.G. Velarde, J. Comput. Appl. Math. 233 (2010) 1432.
[37] M.G. Velarde, W. Ebeling, A.P. Chetverikov, Eur. Phys. J. B 85 (2012) 291.
[38] A.P. Chetverikov, W. Ebeling, M.G. Velarde, Eur. Phys. J. - Special Top. 222 (2013) 2531.
[39] M.G. Velarde, Chetverikov, A.P. Chetverikov, W. Ebeling, E.G. Wilson, K.J. Donovan, Europhys. Lett. 168 (2014) 27004.
[40] A.P. Chetverikov, W. Ebeling, V.D. Lakhno, M.G. Velarde, Phys. Rev. E 100 (2019) 052203.
[41] R.P.G. McNeil, M. Kataoka, C.J.B. Ford, C.H.W. Barnes, D. Anderson, G.A.C. Jones, I. Farrer, D.A. Ritchie, Nature 477 (2011) 439–442.
[42] C.H.W. Barnes, J.M. Shilton, A.M. Robinson, Phys. Rev. B 62 (2000) 8410.
[43] M.R. Astley, M. Kataoka, C.J.B. Ford, C.H.W. Barnes, D. Anderson, G.A.C. Jones, I. Farrer, D.A. Ritchie, M. Pepper, Phys. Rev. Lett. 99 (2007) 156802.
[44] H. Sanada, T. Sogawa, H. Gotoh, K. Onomitsu, M. Kohda, J. Nitta, P.V. Santos, Phys. Rev. Lett. 106 (2011) 216602.
[45] M.R. Astleya, M. Kataokaa, C.J.B. Forda, C.H.W. Barnesa, D. Andersona, G.A.C. Jonesa, I. Farrera, D.A. Ritchiea, M. Peppera, Physica E 40 (2008) 1136.
[46] Stefan Volk, Florian J.R. Schülein, Florian Knall, Dirk Reuter, Andreas D. Wieck, Tuan A. Truong, Hyochul Kim, Pierre M. Petroff, Achim Wixforth, Hubert J. Krenner, Nano Lett. 10 (2010) 3399.
[47] Florian J.R. Schülein, Kai Müller, Max Bichler, Gregor Koblmüller, Jonathan J. Finley, Achim Wixforth, Hubert J. Krenner, Phys. Rev. B 88 (2013) 085307.
[48] A. Ranciaro Neto, M.O. Sales, F.A.B.F. de Moura, Solid State Commun. 229 (2016) 22.
[49] V. Miseikis, J.E. Cunningham, K. Saeed, R. O'Rorke, A.G. Davies, Appl. Phys. Lett. 100 (2012) 133105.
[50] S. Takada, H. Edlbauer, H.V. Lepage, et al., Nature Commun. 10 (2019) 4557.
[51] Hermann Edlbauer, Junliang Wang, Shunsuke Ota, Aymeric Richard, Baptiste Jadot, Pierre-André Mortemousque, Yuma Okazaki, Shuji Nakamura, Tetsuo Kodera, Nobu-Hisa Kaneko, Arne Ludwig, Andreas D. Wieck, Matias Urdampilleta, Tristan Meunier, Christopher Bäuerle, Shintaro Takada, Appl. Phys. Lett. 119 (2021) 114004.

[52] Christopher Bäuerle, et al., Rep. Progr. Phys. 81 (2018) 056503.
[53] J. Holanda, D.S. Maior, A. Azevedo, et al., Nat. Phys. 14 (2018) 500–506.
[54] R. Sasaki, Y. Nii, Y. Onose, Nature Commun. 12 (2021) 2599.
[55] T. Fukuhara, P. SchauB, M. Endres, et al., Nature 502 (2013) 76–79.
[56] Zijian Xiong, Trinanjan Datta, Kenneth Stiwinter, Dao-Xin Yao, Phys. Rev. B 96 (2017) 144436.
[57] Xiaoou Zhang, Yinhan Zhang, Satoshi Okamoto, Di Xiao, Phys. Rev. Lett. 123 (2019) 167202.
[58] Junxue Li, Haakon T. Simensen, Derek Reitz, Qiyang Sun, Wei Yuan, Chen Li, Yaroslav Tserkovnyak, Arne Brataas, Jing Shi, Phys. Rev. Lett. 125 (2020) 217201.
[59] Hiroki Hayashi, Kazuya Ando, Phys. Rev. Lett. 121 (2018) 237202.
[60] Xu Mingran, Yamamoto Kei, Puebla Jorge, Baumgaertl Korbinian, Rana Bivas, Miura Katsuya, Takahashi Hiromasa, Grundler Dirk, Maekawa Sadamichi, Otani Yoshichika, Sci. Adv. 6 (32) (2020).
[61] M. Xu, J. Puebla, F. Auvray, B. Rana, K. Kondou, Y. Otani, Phys. Rev. B. 97 (2018) 180301.
[62] M. Weiler, H. Huebl, F.S. Goerg, F.D. Czeschka, R. Gross, S.T.B. Goennenwein, Phys. Rev. Lett. 108 (2012) 176601.
[63] Yi Li, Chenbo Zhao, Wei Zhang, Axel Hoffmann, Valentyn Novosad, APL Mater. 9 (2021) 060902.
[64] H. Man, Z. Shi, G. Xu, Y. Xu, X. Chen, S. Sullivan, J. Zhou, K. Xia, J. Shi, P. Dai, Phys. Rev. B 96 (2017) 100406, (R).
[65] F. Godejohann, A.V. Scherbakov, S.M. Kukhtaruk, A.N. Poddubny, D.D. Yaremkevich, M. Wang, A. Nadzeyka, D.R. Yakovlev, A.W. Rushforth, A.V. Akimov, et al., Phys. Rev. B 102 (2020) 144438.
[66] A. Rückriegel, P. Kopietz, D.A. Bozhko, A.A. Serga, B. Hillebrands, Phys. Rev. B 89 (2014) 184413.
[67] S. Zhang, G. Go, K.-J. Lee, S.K. Kim, Phys. Rev. Lett. 124 (2020) 147204.
[68] T. Yokouchi, S. Sugimoto, B. Rana, S. Seki, N. Ogawa, S. Kasai, Y. Otani, Nat. Nanotechnol. 15 (2020) 361.
[69] M.O. Sales, A. Ranciaro Neto, F.A.B.F. de Moura, Phys. Rev. E 98 (2018) 062136.
[70] D. Morais, F.A.B.F. de Moura, W.S. Dias, Phys. Rev. B 103 (2021) 195445.
[71] S.N. Evangelou, D.E. Katsanos, Phys. Lett. A 164 (1992) 456.
[72] F.A.B.F. de Moura, M.D. Coutinho-Filho, E.P. Raposo, M.L. Lyra, Phys. Rev. B 66 (2002) 014418.
[73] D. Hennig, A. Chetverikov, M.G. Velarde, W. Ebeling, Phys. Rev. E. 76 (2007) 046602.
[74] K. Ikeda, Y. Doi, B.F. Feng, T. Kawahara, Physica D 225 (2007) 184–196.
[75] E.F. de Lima, R.E. de Carvalho, Physica D 241 (2012) 1753–1757.
[76] J.A. Carrillo, S. Martin, V. Panferov, Physica D 260 (2013) 112–116.
[77] Dm. M. Korotin, V.V. Mazurenko, V.I. Anisimov, S.V. Streltsov, Phys. Rev. B 91 (2015) 224405.
[78] S.K. Satija, J.D. Axe, G. Shirane, H. Yoshizawa, K. Hirakawa, Phys. Rev. B 21 (1980) 2001.
[79] M.T. Hutchings, J.M. Milne, H. Ikeda, J. Phys. C 12 (1979).
[80] Shozo Kadota, Isao Yamada, Shin Yoneyama, Kinshiro Hirakawa, J. Phys. Soc. Japan 23 (1967) L739.
[81] F.A.B.F. de Moura, Int. J. M. Phys. C 22 (2011) 63.
[82] E. Hairer, S.P. Nørsett, G. Wanner, Solving ordinary dierential equations I: Nonstiff problems, in: Springer Series in Computational Mathematics, W. H. Press, B.P. Flannery S.A. Teukolsky and W. T. Wetterling Numerical Recipes, The Art of Scientific Computing, third ed., Cambridge University Press, New York, 2007.
[83] A. Ranciaro Neto, F.A.B.F. de Moura, Commun. Nonlinear Sci. Numer. Simul. 40 (2016) 6.